



Image stacking approach to increase sensitivity of fluorescence detection using a low cost complementary metal-oxide-semiconductor (CMOS) webcam

Joshua Balsam^{a,b}, Hugh Alan Bruck^b, Yordan Kostov^c, Avraham Rasooly^{a,d,*}

^a Division of Biology, Office of Science and Engineering, FDA, Silver Spring, MD 20993, United States

^b University of Maryland College Park (UMCP), College Park, MD 20742, United States

^c Center for Advanced Sensor Technology, University of Maryland Baltimore County, MD 21250, United States

^d National Cancer Institute, Bethesda, MD 20892, United States

ARTICLE INFO

Article history:

Received 6 September 2011

Accepted 2 February 2012

Available online 23 May 2012

Keywords:

Webcam

Image stacking

CMOS

CCD

LED

Fluorescence

Fluorometer

Global health

ABSTRACT

Optical technologies are important for biological analysis. Current biomedical optical analyses rely on high-cost, high-sensitivity optical detectors such as photomultipliers, avalanched photodiodes or cooled CCD cameras. In contrast, Webcams, mobile phones and other popular consumer electronics use lower-sensitivity, lower-cost optical components such as photodiodes or CMOS sensors. In order for consumer electronics devices, such as webcams, to be useful for biomedical analysis, they must have increased sensitivity. We combined two strategies to increase the sensitivity of CMOS-based fluorescence detector.

1. We captured hundreds of low sensitivity images using a Webcam in video mode, instead of a single image typically used in cooled CCD devices.
2. We then used a computational approach consisting of an image stacking algorithm to remove the noise by combining all of the images into a single image.

While video mode is widely used for dynamic scene imaging (e.g. movies or time-lapse photography), it is not used to capture a single static image, which removes noise and increases sensitivity by more than thirty fold. The portable, battery-operated Webcam-based fluorometer system developed here consists of five modules: (1) a low cost CMOS Webcam to monitor light emission, (2) a plate to perform assays, (3) filters and multi-wavelength LED illuminator for fluorophore excitation, (4) a portable computer to acquire and analyze images, and (5) image stacking software for image enhancement. The samples consisted of various concentrations of fluorescein, ranging from 30 μM to 1000 μM , in a 36-well miniature plate. In the single frame mode, the fluorometer's limit-of-detection (LOD) for fluorescein is $\sim 1000 \mu\text{M}$, which is relatively insensitive. However, when used in video mode combined with image stacking enhancement, the LOD is dramatically reduced to 30 μM , sensitivity which is similar to that of state-of-the-art ELISA plate photomultiplier-based readers. Numerous medical diagnostics assays rely on optical and fluorescence readers. Our novel combination of detection technologies, which is new to biodetection may enable the development of new low cost optical detectors based on an inexpensive Webcam (<\$10). It has the potential to form the basis for high sensitivity, low cost medical diagnostics in resource-poor settings.

Published by Elsevier B.V.

1. Introduction

Optical detection is the most common approach used in research, clinical and industrial laboratory analysis. Several optical detection methods developed for biodetection employ photodiodes [1–4] and photomultipliers [5–10], which are inherently highly

sensitive spot detectors for analysis of limited areas. As an alternative, charged-coupled devices (CCDs) [10–18] have been used for spatial detection to monitor larger surface areas which made them an ideal choice for multichannel detection, since many sample channels can be analyzed simultaneously. Several portable CCD-based detection systems have been developed [19–26] based on single image capturing and analysis. Such detectors have sensitivity similar to that of current laboratory ELISA readers utilizing sensitive research grade cameras [19,20,27] or astronomical cooled CCD cameras [21–26]. While photomultipliers are far more sensitive than cooled CCD cameras, the longer exposure of cooled CCD

* Corresponding author at: NIH/NCI, 6130 Executive Blvd. EPN, Room 6035A, Rockville, MD 20852, United States. Tel.: +301 402 4185; fax: +301 402 7819.

E-mail address: rasoolya@mail.nih.gov (A. Rasooly).

cameras compensates for their lower sensitivity [21–26]. However, cooled CCD devices are costly, which limits their use in resource-poor settings around the world.

There have been some notable recent developments in technologies that are suitable for low resource healthcare systems. Low cost microscopy was developed to address global health needs utilizing lens free approaches [28–36] and mobile cell phones have been adapted for biodetection [37–41]. These devices are based on low cost complementary metal-oxide-semiconductor (CMOS) sensors which are also used in Webcam video cameras developed for home video imaging. They feed video images in real-time to a computer. The fundamental issue that needs to be addressed in order for Webcams to be used for biodetection is the low sensitivity of the CMOS Webcam.

One approach, described here, is to use multiple video captured images combined with stacking for image enhancement. While video mode is widely used for dynamic scene imaging, it has not been used for capturing a single static image, and the use of image stacking on multiple video captured images was not reported previously for biodetection. A digital image consists of large number of pixels, and for color CCD and CMOS, each pixel contains three channels (red, blue and green). In video mode, many compressed images (e.g. 30 frames per second) are captured from the camera. Using image stacking software, it is possible to calculate the average value of each pixel for a series of video frames in order to generate an averaged single image. Each pixel in an individual frame may contain a signal and/or noise and compression artifacts. Therefore, the random noise present in each frame will be reduced toward zero after image stacking, while the signal present in all frames will be preserved as a constant value in the averaged combined single image. Thus, image stacking enables the removal of random noise and compression artifacts from a series of video images, creating a clear single static image with a significantly improved signal-to-noise ratio (SNR). What we have been able to establish for the first time is the relationship between the image stacking of the video captured images from the Webcam and the improvement in the SNR.

Based on these findings, low cost and sensitive detection devices can be developed to bring modern sensitive diagnostics to many underserved populations all around the world.

2. Experimental

2.1. Materials and reagents

The 36-well chips used for analysis were fabricated using 1/8 in. black poly(methyl methacrylate) (PMMA) also known as acrylic and polycarbonate (PC) (Piedmont Plastic Inc., Beltsville, MD) bonded with 3M 9770 adhesive transfer double sided tape (Piedmont Plastic Inc., Beltsville, MD).

2.2. Webcam-based fluorescence detector

The details of our optical design for biodetection are described in previous work on cooled CCD detection [21,42,43], here we replaced the high cost, low noise sensitive cooled CCD with a low cost Webcam. The Webcam based fluorometer consists of a multi spectra LED light source [42], blue excitation D486/10X and green emission HQ535/50M filters (Chroma Technology Corp., Rockingham, VT), and a generic Webcam color video camera (AVEO Corp) with a 8 bit 640×480 pixel CMOS enabling 256 levels of gray scale (typical Ebay vendor). As in many Webcams, the exposure time is determined automatically based on the light reaching the CMOS, and cannot be controlled by the user. The original lens of the Webcam is a fixed aperture, fixed focal length, with variable focus. For our measurements, we first used the original 5 mm, f3.8 lens, and

then removed the lens and attached a Tamron manual zoom CCTV 4–12 mm, f1.2 lens (Spytown, Utopia, NY).

The Webcam was compared to a black and white Meade Deep Sky Imager PRO™ III CCD astronomical camera (Adirondack Video Astronomy, Hudson Falls, NY) equipped with a Sony ICX-285AL 1360×1024 pixel, the 16 bit CCD enables 65,000 gray scale levels using similar configuration as the CMOS. The camera was equipped with the Tamron manual zoom CCTV 4–12 mm, f1.2 lens. Both detectors were connected to a Windows XP PC via a USB port.

2.3. Video image analysis

Images for both platforms single frame for CCD and video file for Webcam were captured using software supplied by the manufacturer: CamApp v. 1.0.0.9 (Aveo Corp., 2008), and AutoStar Envisage v. 7.03 (Meade Instruments Corp., 2007). The CMOS and CCD image intensities were analyzed using ImageJ software, developed and distributed freely by NIH (<http://rsb.info.nih.gov/ij/download.html>). Then, the data generated is imported into Microsoft Excel (Microsoft, Redmond, WA) for further manipulation. A SPA-RP Reflectance Probe spectrometer was used for spectra analysis.

The incoming video stream from the Webcam is enhanced using a software-based video processing amplifier built into the CamApp software. The brightness adjustment applies a uniform shift to the luminance values of all pixels causing a uniform (i.e. scalar) increase in measured luminance. The brightness setting is chosen such that no pixels are recorded as having a luminance value of zero or maximum (for an 8-bit image this corresponds to values of 0 or 255). Because all pixels are generating a signal (due either to photons or to on-chip sources of noise), if any pixels in the image are recorded as having zero signal it means that signal is being lost. Increasing all pixel values in this manner inherently causes a uniform decrease in the signal-to-noise ratio (SNR) not representative of improved imaging quality. Therefore, this uniform increase in all pixel values is subtracted later during image processing in order to recover the original SNR and provide the opportunity to use other image adjustments that may increase the signal non-uniformly without saturating the image.

The contrast adjustment applies a non-uniform adjustment to the luminance of each pixel. This adjustment is a function of the pixel luminance value: the luminance of darker pixels is increased slightly, while the luminance of the brighter pixels is increased more (i.e. SNR is increased with higher contrast settings). Therefore, unlike the brightness, the contrast setting is set to a maximum value since the signal being detected will be at higher luminance values.

The goal of the brightness and contrast adjustment is to force the range of the recorded pixel values to be as large as possible to take advantage of dynamic range afforded by the 8-bit sensor (i.e. to broaden the histogram). In the final recorded image, the luminance of the darkest pixels should be close to zero and that of the brightest should be as high as possible without being saturated.

Other image processing operations, such as gamma correction and sharpness, can introduce nonlinear or highly localized adjustments to the luminance function. Both gamma and sharpness were set to zero to minimize unnecessary or biased manipulation of the data stream.

Images from the Webcam were captured using two methods: single frame and video. Single frame capture is identical to the operation of a conventional camera. Exposure time is governed by an onboard controller, and has a lower limit of approximately 1/30 s (dictated by frame rate). In video mode, a stream of frames is captured for 10–15 s and saved as a compressed AVI file. At thirty frames per second, this amounts to several hundred frames. This file is then split into its constituent frames and averaged together

through image stacking via ImageJ software. Thus, averaging serves to reduce the effects of random variation in the signal due to noise.

In both cases one image is obtained with the excitation light turned on and the sample in place (a 'light frame'). The excitation source is then turned off and another frame is captured (a 'dark frame'). The dark frame records any background noise from the sensor (thermal noise, etc.). The dark frame is subtracted from the light frame to remove this background noise and improve the SNR. Image subtraction and measurement is performed with ImageJ, and the data generated is then imported into Microsoft Excel for statistical analysis. The limit of detection (LOD) can then be established by taking the average signal of a control (water) and adding 3 times the standard deviation to it.

2.4. Fabrication of the 36-well sample fluidics

The details of our laser fabrication of LOC for assay measurement are described in previous work [24,25,43,44], the 36-well sample chips used in this study were designed in CorelDraw X4 (Corel Corp., Ontario, Canada) and then micro-machined in 1/8 in. black acrylic using a computer controlled laser cutter Epilog Legend CO₂ 65W cutter (Epilog, Golden, CO). Before cutting, one side of the acrylic sheets was coated with 3M 9770 adhesive transfer double sided tape.

3. Results and discussion

The Webcam CMOS-based fluorometer described in this study was designed with the aim of utilizing the video capture abilities of low sensitivity CMOS in combination with a computational image enhancement, in order to improve the sensitivity of low cost optical biodetection.

The main challenges of replacing sensitive CCD cameras with Webcams are: (1) the thermal noise (dark current) produced by having electrons generated by physical processes within the CMOS sensor itself rather than by the absorption of photons (i.e. the signal) is far greater than in advanced CCD cameras, reducing significantly the sensitivity of low cost Webcams. (2) Unlike advanced CCD cameras which enable the user to set exposure time, in low cost Webcams exposure time is determined automatically based on the light exposure of the CMOS sensor, and cannot be controlled by the user. (3) While advanced CCD cameras permit long exposures (e.g. an hour or more), the exposure time for Webcams is very short (e.g. 1/30 s). (4) The original lens for low cost Webcams is a fixed aperture limiting the ability to control the light or to increase the amount of light reaching the CMOS sensor.

In order to adapt Webcams for biosensing, these challenges must be overcome.

3.1. Webcam CMOS-based fluorometer

The basic configuration of the Webcam CMOS-based fluorometer is shown schematically in Fig. 1A. The system consists of four main elements (described in more detail below): (a) the CMOS detector module, (b) the assay chip module, (c) the illumination/excitation module, and (d) a computer to acquire and analyze images.

The LED illumination module [42] is comprised of a custom built multi-wavelength LED illumination box and the Excitation Filter. The multi-wavelength LED illumination box equipped with RGB LED can illuminate with red, green, blue or white spectra (Fig. 1C) capable of exciting multiple fluorophores. However, only illumination in the blue range is needed for the fluorescein excitation used in this study (Fig. 1D). The LED illuminator contains four RGB LED strips and four daylight LED strips for white illumination, both types of strips consisting of 18 LEDs per foot. Each LED color is controlled

individually with a switch in the front panel, the top of the illuminator consists of a diffusion panel (milky white plastic panel), which assures uniformity of the LED light. As shown in Fig. 1C, the multi-wavelength LED illumination box provides broad spectra illumination in the blue, green, red, and white ranges, covering a spectrum of 450–650 nm (red 610–650 nm, green 512–550 nm, and blue 450–465 nm). The fluorescein measured in this work has a peak excitation wavelength of 494 nm and an emission maximum of 521 nm. For this work, we used the blue LED, which emits in the range of 420–550 nm (Fig. 1C) with a peak at ~470 nm. The broad emission spectra of the blue LED overlaps with the fluorescein emission (Fig. 1C), therefore to minimize the "noise" a blue pass filter D486/10X with a very narrow range of ~475–490 nm (Fig. 1D) was used for fluorescein excitation and a green pass filter HQ535/50M with a range of ~525–540 nm was used for fluorescein emission.

In our optical configuration (Fig. 1A) the excitation source is directly in line with the CCD, so the excitation and emission filters are crucial for blocking any excitation light reaching the detector, while still allowing the fluorescence emission to be transmitted. There is no detectable overlap between the spectra of the blue and the green filters, when the two filters are combined and illuminated by the blue LED, no signal is detected suggesting very little blue "noise" can reach the CMOS.

We used a generic webcam camera, which consisted of a simple, low-cost 8 bit CMOS camera powered by a USB2 port, so it can be operated by a computer battery for field use. The USB2 port also enables fast data transmission, and can be controlled with Labview software, allowing for simple system automation.

The interchangeable laminated assay module enables analysis of small volumes (~30 µl). It is a two layer microfluidic structure consisting of a rigid polymer core (e.g. 3.2 mm black poly(methyl methacrylate) (PMMA)) that is laminated with layers of thin polymer (e.g. polycarbonate (PC) film) bonded with adhesive. The relatively thick black core provides rigidity to the assembly and the black color minimizes optical crosstalk between the wells.

3.2. Webcam detection of fluorescein

To study the capabilities of the CMOS-based Webcam fluorometer equipped with the original 5 mm f3.8 lens, serial dilutions of fluorescein (a common dye used in many biological assays) in the range of 0–1 mg/ml were analyzed. Fig. 2 shows the emission image of six concentrations of fluorescein (0 µM (water) to 500 µM) loaded into the 36-well sample chip (rows 1–6 in Fig. 2A) in six replicas (columns a–f in Fig. 2A) recorded with the Webcam and analyzed with ImageJ software.

As shown in Fig. 2A, there is no visible signal in the control (water, row #6) except row 6 column e (marked with a circle) a reference point which can be used to orient the plate. A signal is detected for the 500 µM (row #1).

The resulting CMOS images were analyzed in ImageJ which allows the user to quantify the intensity from user-specified areas of the image. A 3D ImageJ analysis is shown in Fig. 2B, in which the signal level for each well corresponds to the concentration of the fluorescein suggest that there is no strong signal except for the 500 µM (rows 1). The LOD was determined to be 1000 µM.

As in any imaging device, the lens plays a major role in image quality. To increase sensitivity of the camera, we substituted the original 5 mm f3.8 lens of the Webcam with a Tamron manual zoom CCTV 4–12 mm, f1.2 lens. Samples of varying concentrations of fluorescein in the same range (0–500 µg/ml) were analyzed with this lens (Fig. 2C). The corresponding 3D ImageJ analysis (Fig. 2D) clearly indicates higher signals corresponding to 500 µM.

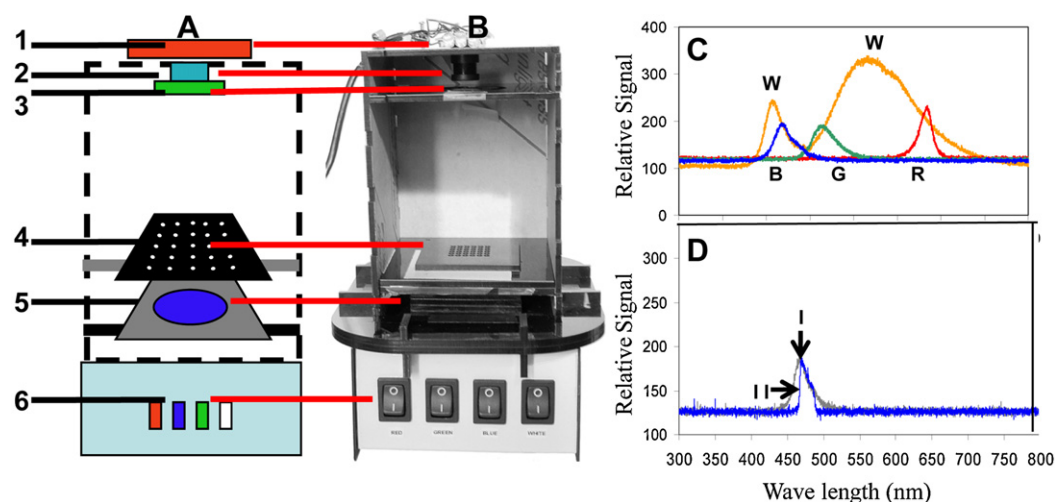


Fig. 1. Webcam-based fluorometer. (A) A schematic configuration of the Webcam-based fluorometer with the main system components highlighted in the schematic: (1) a Webcam camera mounted in a homemade acrylic box, (2) interchangeable lens [with a green band pass emission filter], (3) mounted on the end of the lens. Black acrylic sample chip (4). Blue band pass excitation filter (5) and multi-wavelength LED (6). (B) A photo of a Webcam-based fluorometer. (C) The excitation spectra (measured by a spectrometer) of the multi-wavelength LED for the white, W, blue, B, green, G, and red, R, LED illumination. (D) Blue LED illumination spectra with, I, or without, II, blue filter. (For interpretation of the references to color in this figure legend, the reader is referred to the web version of this article.)

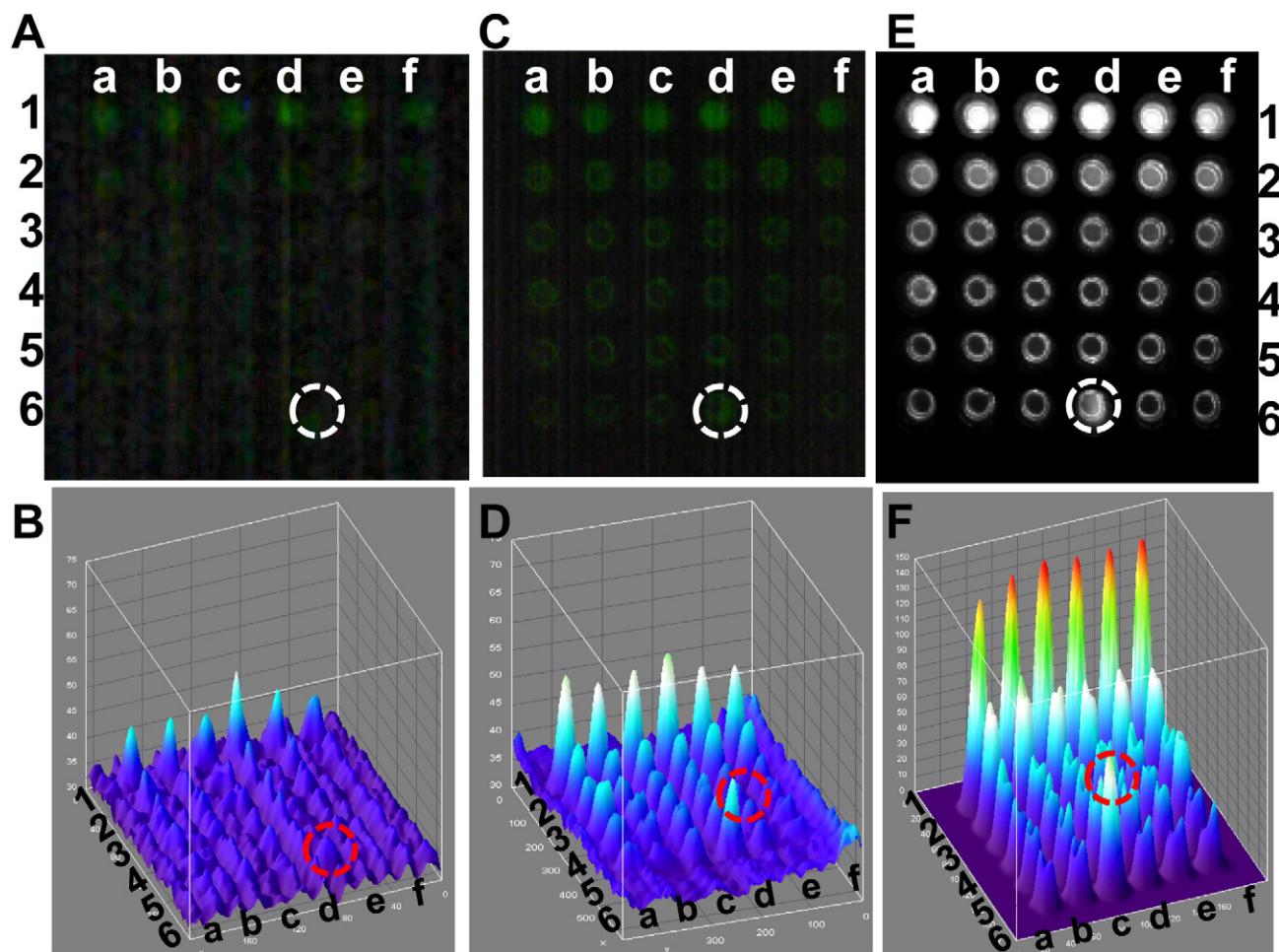


Fig. 2. Webcam detection of fluorescein. A thirty six well plate was loaded with six concentrations of fluorescein (rows 1–6) each in six replicas (columns a–f). The plate was illuminated by a blue LED equipped with a blue excitation filter and the plate was measured with a green emission filter. The signals of the wells were detected by (A) CMOS Webcam equipped with the original f3.8 5 mm lens and the corresponding ImageJ 3D image is shown in (B). The CMOS Webcam image with a Tamron manual zoom CCTV 4–12 mm, f1.2 lens and is shown in (C) with the corresponding ImageJ 3D image in (D). The image of CCD camera equipped with the zoom lens (E) and the corresponding ImageJ 3D image (F). The fluorescein concentrations used: row #1: 500 μ M, row #2: 250 μ M, row #3: 125 μ M, row #4: 60 μ M, row #5: 30 μ M and row #6: control (water). Row 5 column e (marked with a circle) is a reference point which can be used to orient the plate. (For interpretation of the references to color in this figure legend, the reader is referred to the web version of this article.)

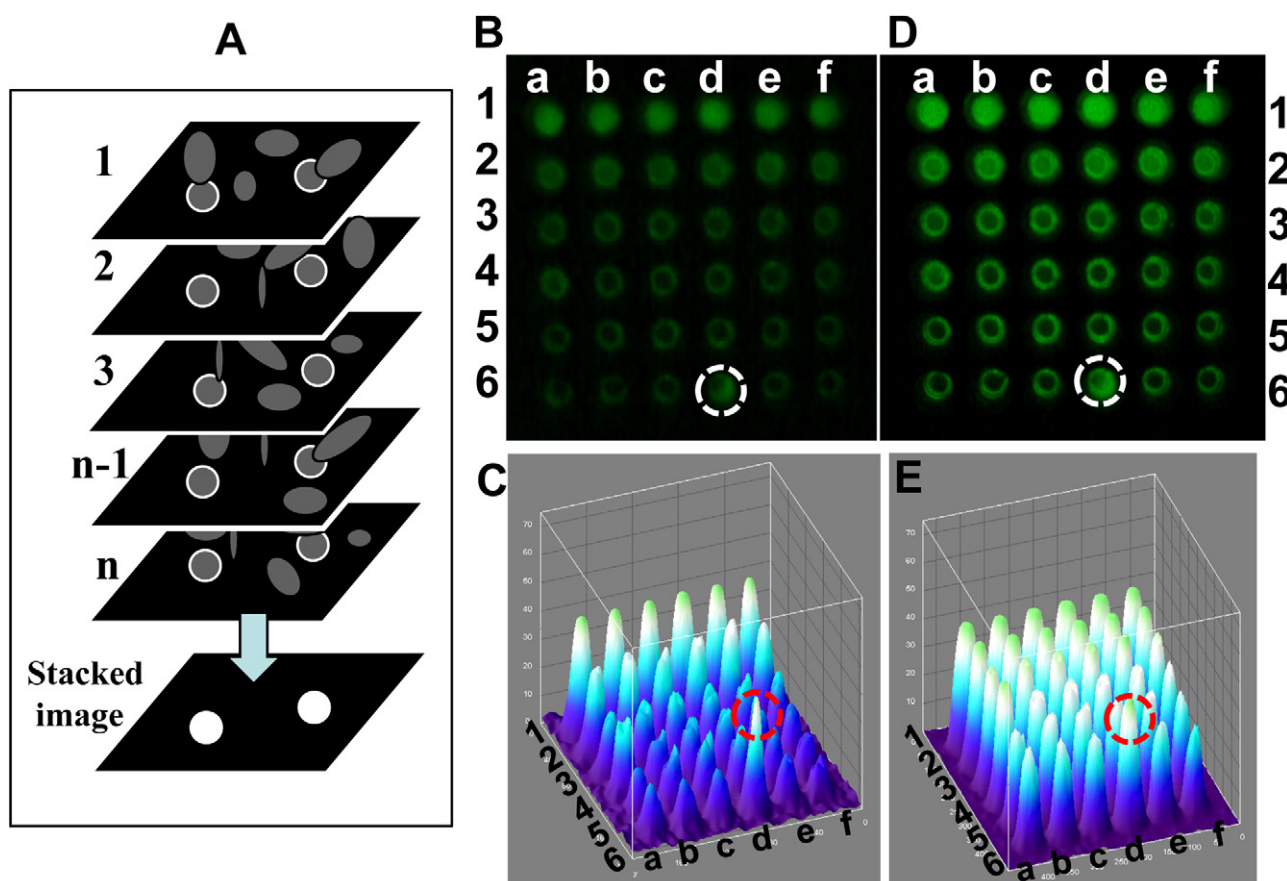


Fig. 3. Image enhancement of Webcam video captured images. A schematic of image stacking for enhanced imaging is shown in (A); the Webcam in video mode captures n individual frames. In each frame there are pixels with a signal (marked with white circle) and pixels with random noise (gray). In the individual frames it is difficult to distinguish between the signal and the noise. In the stacked image, which contains the average value of each pixel for all frames, the random noise present in each frame will be significantly reduced and only the signal will be present in the averaged single image resulting in enhanced signal-to-noise ratio (SNR). The thirty six well plate was loaded with six concentrations of fluorescein (rows 1–6) each in six replicas (columns a–f). The plate was illuminated by a blue LED equipped with a blue excitation filter, and the plate was measured with a with a green emission filter. The signals of the wells were detected by the CMOS Webcam equipped with the original f3.8 5 mm lens operating in a video mode and enhanced by image stacking (B), the corresponding ImageJ 3D image is shown in (C). The enhanced image of the CMOS Webcam image with a Tamron manual zoom CCTV 4–12 mm, f1.2 lens is shown in (D) with the corresponding ImageJ 3D image in (E). The fluorescein concentrations used: row #1: 500 μM , row #2: 250 μM , row #3: 125 μM , row #4: 60 μM , row #5: 30 μM and row #6: control (water). Row 5 column d (marked with a circle is a reference point which can be used to orient the plate). The signal-to-noise ratio (SNR) for all detectors was plotted against the various fluorescein concentrations.

A similar optical configuration to that shown in Fig. 1 as used for CCD-based detection of fluorescein to compare with the CMOS camera. The CCD camera used in this experiment is a sensitive astronomy grade Mead Deep Sky Imager PRO III CCD camera equipped with a monochrome 16 bit Sony ICX-285AL 1360 \times 1024 pixel CCD and a Tamron manual zoom CCTV 4–12 mm f1.2 lens. As shown in Fig. 2E, the signals in the CCD image are significantly higher than the Webcam signals using the same f1.2 lens, as shown clearly in the 3D image (Fig. 2F). The LOD for the CCD analysis was 30 μM , which was more than one order of magnitude more sensitive than the Webcam.

Four factors contribute to the CCD performance: (1) the high sensitivity of the CCD, (2) the fact that it is a 16 bit device enable broad dynamic range of 65,500 levels of grayscale compared to the 8 bit CMOS with only 256 level grayscale, (3) that it is a monochrome CCD which uses the whole pixel while the color CMOS is divided into a square of four pixels consisting of one filtered red, one blue, and two green which decreasing the effective detection area of the pixel by 1/4th, and (4) unlike the Webcam, the exposure time in the CCD camera can be controlled from 1/10,000th s to 1 h enabling more light into the CCD and thus increase the sensitivity. However, in this sensitive detector the limiting factor is the noise (e.g. residual green light from the blue LED not filtered by the blue filter), and not the CCD or the lens.

3.3. Image enhancement of Webcam video captured images

The astronomy grade CCD camera is superior to the Webcam but the cost of such camera is $\sim 100\times$ greater than the Webcam making it impractical for low cost Global Health applications. One way to increase the Webcam sensitivity is to digitally improve the image. Since the Webcam was designed to be a video camera, capturing many hundreds of frames and using them to compile a single image ("stacking" the video frames) can be used reduce the noise and improve image quality.

A schematic of image stacking for enhanced imaging is shown in (Fig. 3A); the Webcam in video mode captures n individual frames. In each frame there are pixels with a signal (marked with white circle) and pixels with random noise. In the individual frames it is difficult to distinguish between the signal and the noise. In the stacked image, which contains the average value of each pixel for all frames, the random noise present in each frame will be significantly reduced and only the signal will be present in the averaged single image resulting in an enhanced SNR.

To measure the effectiveness of image stacking to improve CMOS measurement sensitivity, the thirty six well plate was loaded with six concentrations of fluorescein (rows 1–6) each in six replicas (columns a–f). The plate was illuminated by a blue LED equipped with a blue excitation filter, and the plate was measured with a with

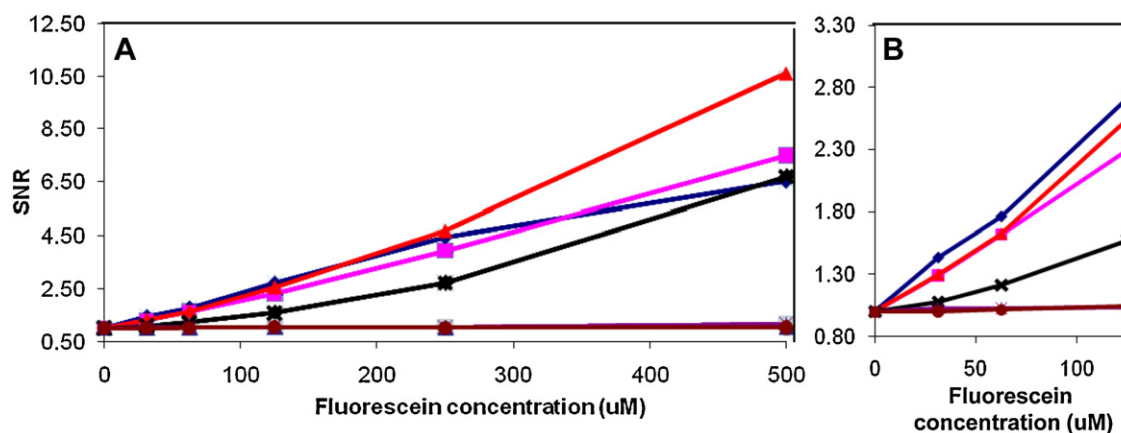


Fig. 4. A comparison of fluorescein detection between Webcam, CCD camera and plate reader. The signal-to-noise ratio (SNR) for all three detectors was plotted against the various fluorescein concentrations. (A) The whole range of concentrations 0–500 μM and (B) a plot of the lower concentrations 0–120 μM . Triangle, CCD camera with f1.2 lens. Square, Webcam equipped with f3.8 lens after image enhancement. Diamond, Webcam equipped with f1.2 lens after image enhancement. X, plate reader; star, Webcam equipped with f1.2 lens (no image enhancement); circle, Webcam equipped with f3.8 lens (no image enhancement).

a green emission filter. The signals of the wells were detected by the CMOS Webcam equipped with the original f3.8 5 mm lens operating in a video mode and enhanced by image stacking (Fig. 3B) the corresponding ImageJ 3D image (Fig. 3C) clearly shows a very good signal indicating a LOD of 60 μM . The enhanced image of the CMOS Webcam image with a Tamron manual zoom CCTV 4–12 mm, f1.2 lens (Fig. 3D) shows even better sensitivity as shown in the 3D analysis (Fig. 3E). The LOD for this measurement is 30 μM , which is similar to the CCD measurements.

We compared our measurement with the measurement of a conventional plate reader. The LOD of the plate reader is 60 μM which is similar to the Webcam with the f3.8 lens. A plot of all the measurements is shown in Fig. 4. It clearly shows that in low concentrations, where LOD is most important, the Webcam with the f1.2 lens performs the best. It outperforms the plate reader at all concentration levels, and only falls short of the CCD at higher concentrations (Fig. 4A).

4. Conclusion

To overcome the limitations of low sensitivity in a Webcam, we combined two strategies that increased its sensitivity to enable it to be used as CMOS based fluorescence detector for biological analysis. First, we captured hundreds of low sensitivity images using a Webcam in video mode, instead of a single image typically used in cooled CCD devices, and then used a computational approach consisting of an image stacking algorithm to remove the noise from the many images and combine them into a single image with a thirty fold reduction in the SNR. Video mode is very widely used for dynamic scene imaging (e.g. movies or time-lapse photography), however it is not used to capture a single static image, so the novel use of video mode for still imaging significantly increases the sensitivity of the Webcam. Using the CMOS Webcam fluorometer enabled detection of 1000 μM with the original f3.8 lens and 500 μM with f1.2 lens, the use of video mode and the stacking software increased the sensitivity by nearly thirty folds, resulting in a sensitivity similar to a CCD camera or a plate reader. This suggests that with image stacking the most basic, simple, and lowest cost Webcam can provide sensitivity similar or superior to a sophisticated state-of-the-art plate reader.

Many labs, including ours, have been developing various low-cost diagnostic Point of Care (POC) technologies for resource-poor settings with minimal medical infrastructure. By using inexpensive (e.g. \$10) Webcams combined with the image stacking software for biodetection it may be possible to better utilize POC technologies

in global health settings. Because the Webcam is a simple low-cost device available in resource poor regions, it may be practical to develop a Webcam-based fluorometer for telemedicine and global health application for ~\$100 with the sensitivity and capacity to detect multiple analytes, as well as the high throughput capabilities of modern quantitative diagnostics not currently available in a global health setting. Such detectors may enable the performance of many medical diagnostics assays used today, ranging from various immunoassays and microbial analyses used in food and water safety application to cardiovascular and cancer diagnostics, that all rely on optical and fluorescence detection. Moreover, beyond the Webcam-based fluorometer, the approach described here can be used for many other biomedical devices based on optical detection ranging from microarray analysis to flow cytometry, and thus may bring current medical diagnostics approaches to the majority of the world's population who do not have access to medical diagnostics.

Funding

Funded by the National Cancer Institute, Cancer Diagnosis Program and the FDA's Center for Devices and Radiological Health, Office of Science and Engineering, Division of Biology.

References

- [1] L.F. Capitan-Vallvey, L.J. Asensio, J. Lopez-Gonzalez, M.D. Fernandez-Ramos, A.J. Palma, Oxygen-sensing film coated photodetectors for portable instrumentation, *Analytica Chimica Acta* 583 (2007) 166–173.
- [2] M.M. Mac Sweeney, C. Bertolino, H. Berney, M. Sheehan, Characterization and optimization of an optical DNA hybridization sensor for the detection of multi-drug resistant tuberculosis, in: *Conference Proceedings – IEEE Engineering in Medicine and Biology Society*, vol. 3, 2004, pp. 1960–1963.
- [3] R.W. Claycomb, M.J. Delwiche, Biosensor for on-line measurement of bovine progesterone during milking, *Biosensors and Bioelectronics* 13 (1998) 1173–1180.
- [4] A.E. Bruno, S. Barnard, M. Rouilly, A. Waldner, J. Berger, M. Ehrat, All-solid-state miniaturized fluorescence sensor array for the determination of critical gases and electrolytes in blood, *Analytical Chemistry* 69 (1997) 507–513.
- [5] S. Moehrs, A. Del Guerra, D.J. Herbert, M.A. Mandelkern, A detector head design for small-animal PET with silicon photomultipliers (SiPM), *Physics in Medicine & Biology* 51 (2006) 1113–1127.
- [6] M. Takei, T. Kida, K. Suzuki, Sensitive measurement of positron emitters eluted from HPLC, *Applied Radiation and Isotopes* 55 (2001) 229–234.
- [7] M.C. Ruiz-Martinez, J. Berka, A. Belenkii, F. Foret, A.W. Miller, B.L. Karger, DNA sequencing by capillary electrophoresis with replaceable linear polyacrylamide and laser-induced fluorescence detection, *Analytical Chemistry* 65 (1993) 2851–2858.
- [8] A.G. Tibbe, B.G. de Grooth, J. Greve, P.A. Liberti, G.J. Dolan, L.W. Terstappen, Cell analysis system based on immunomagnetic cell selection and alignment

- followed by immunofluorescent analysis using compact disk technologies, *Cytometry* 43 (2001) 31–37.
- [9] K. Tsukagoshi, N. Jinno, R. Nakajima, Development of a micro total analysis system incorporating chemiluminescence detection and application to detection of cancer markers, *Analytical Chemistry* 77 (2005) 1684–1688.
 - [10] A. Roda, A.C. Manetta, O. Portanti, M. Mirasoli, M. Guardigli, P. Pasini, R. Lelli, A rapid and sensitive 384-well microtitre format chemiluminescent enzyme immunoassay for 19-nortestosterone, *Luminescence* 18 (2003) 72–78.
 - [11] F.S. Ligler, C.R. Taitt, L.C. Shriver-Lake, K.E. Sapsford, Y. Shubin, J.P. Golden, Array biosensor for detection of toxins, *Analytical and Bioanalytical Chemistry* 377 (2003) 469–477.
 - [12] J. Svitel, I. Surugiu, A. Dzgoev, K. Ramanathan, B. Danielsson, Functionalized surfaces for optical biosensors: applications to in vitro pesticide residual analysis, *Journal of Materials Science Materials in Medicine* 12 (2001) 1075–1078.
 - [13] Y. Liu, B. Danielsson, Rapid high throughput assay for fluorimetric detection of doxorubicin—application of nucleic acid-dye bioprobe, *Analytica Chimica Acta* 587 (2007) 47–51.
 - [14] K. Burkert, T. Neumann, J. Wang, U. Jonas, W. Knoll, H. Ottleben, Automated preparation method for colloidal crystal arrays of monodisperse and binary colloid mixtures by contact printing with a pintool plotter, *Langmuir* 23 (2007) 3478–3484.
 - [15] K. Tohda, M. Gratzl, Micro-miniature autonomous optical sensor array for monitoring ions and metabolites 2: color responses to pH, K⁺ and glucose, *Analytical Sciences* 22 (2006) 937–941.
 - [16] M.J. Feldstein, J.P. Golden, C.A. Rowe, B.D. Maccraith, F.S. Ligler, Array biosensor: optical and fluidics systems, *Biomedical Microdevices* 1 (1999) 139–153.
 - [17] Y.S. Sohn, A. Goodey, E.V. Anslyn, J.T. McDevitt, J.B. Shear, D.P. Neikirk, A microbead array chemical sensor using capillary-based sample introduction: toward the development of an electronic tongue, *Biosensors and Bioelectronics* 21 (2005) 303–312.
 - [18] B.G. Knecht, A. Strasser, R. Dietrich, E. Martlbauer, R. Niessner, M.G. Weller, Automated microarray system for the simultaneous detection of antibiotics in milk, *Analytical Chemistry* 76 (2004) 646–654.
 - [19] M.M. Ngundi, S.A. Qadri, E.V. Wallace, M.H. Moore, M.E. Lassman, L.C. Shriver-Lake, F.S. Ligler, C.R. Taitt, Detection of deoxynivalenol in foods and indoor air using an array biosensor, *Environmental Science and Technology* 40 (2006) 2352–2356.
 - [20] F.S. Ligler, K.E. Sapsford, J.P. Golden, L.C. Shriver-Lake, C.R. Taitt, M.A. Dyer, S. Barone, C.J. Myatt, The array biosensor: portable, automated systems, *Analytical Sciences* 23 (2007) 5–10.
 - [21] K.E. Sapsford, S. Sun, J. Francis, S. Sharma, Y. Kostov, A. Rasooly, A fluorescence detection platform using spatial electroluminescent excitation for measuring Botulinum neurotoxin A activity, *Biosensors and Bioelectronics* 24 (2008) 618–625.
 - [22] M. Yang, Y. Kostov, H.A. Bruck, A. Rasooly, Carbon nanotubes with enhanced chemiluminescence immunoassay for CCD-based detection of Staphylococcal enterotoxin B in food, *Analytical Chemistry* 80 (2008) 8532–8537.
 - [23] M. Yang, Y. Kostov, A. Rasooly, Carbon nanotubes based optical immunodetection of Staphylococcal enterotoxin B (SEB) in food, *International Journal of Food Microbiology* 127 (2008) 78–83.
 - [24] K.E. Sapsford, J. Francis, S. Sun, Y. Kostov, A. Rasooly, Miniaturized 96-well ELISA chips for Staphylococcal enterotoxin B detection using portable colorimetric detector, *Analytical and Bioanalytical Chemistry* 394 (2009) 499–505.
 - [25] S. Sun, M. Ossandon, Y. Kostov, A. Rasooly, Lab-on-a-chip for Botulinum neurotoxin A (BoNT-A) activity analysis, *Lab on a Chip* 9 (2009) 3275–3281.
 - [26] M. Yang, Y. Kostov, H.A. Bruck, A. Rasooly, Gold nanoparticle-based enhanced chemiluminescence immunosensor for detection of Staphylococcal enterotoxin B (SEB) in food, *International Journal of Food Microbiology* 133 (2009) 265–271.
 - [27] C.R. Taitt, G.P. Anderson, F.S. Ligler, Evanescent wave fluorescence biosensors, *Biosensors and Bioelectronics* 20 (2005) 2470–2487.
 - [28] A.F. Coskun, I. Sencan, T.W. Su, A. Ozcan, Wide-field lensless fluorescent microscopy using a tapered fiber-optic faceplate on a chip, *Analyst* 136 (2011) 3512–3518.
 - [29] W. Bishara, U. Sikora, O. Mudanyali, T.W. Su, O. Yaglidere, S. Luckhart, A. Ozcan, Holographic pixel super-resolution in portable lensless on-chip microscopy using a fiber-optic array, *Lab on a Chip* 11 (2011) 1276–1279.
 - [30] T.W. Su, S.O. Isikman, W. Bishara, D. Tseng, A. Erlinger, A. Ozcan, Multi-angle lensless digital holography for depth resolved imaging on a chip, *Optics Express* 18 (2010) 9690–9711.
 - [31] C. Oh, S.O. Isikman, B. Khademhosseini, A. Ozcan, On-chip differential interference contrast microscopy using lensless digital holography, *Optics Express* 18 (2010) 4717–4726.
 - [32] O. Mudanyali, D. Tseng, C. Oh, S.O. Isikman, I. Sencan, W. Bishara, C. Oztoprak, S. Seo, B. Khademhosseini, A. Ozcan, Compact, light-weight and cost-effective microscope based on lensless incoherent holography for telemedicine applications, *Lab on a Chip* 10 (2010) 1417–1428.
 - [33] S.O. Isikman, I. Sencan, O. Mudanyali, W. Bishara, C. Oztoprak, A. Ozcan, Color and monochrome lensless on-chip imaging of *Caenorhabditis elegans* over a wide field-of-view, *Lab on a Chip* 10 (2010) 1109–1112.
 - [34] A.F. Coskun, I. Sencan, T.W. Su, A. Ozcan, Lensless wide-field fluorescent imaging on a chip using compressive decoding of sparse objects, *Optics Express* 18 (2010) 10510–10523.
 - [35] O. Mudanyali, A. Erlinger, S. Seo, T.W. Su, D. Tseng, A. Ozcan, Lensless on-chip imaging of cells provides a new tool for high-throughput cell-biology and medical diagnostics, *Journal of Visualized Experiments* (2009).
 - [36] S. Moon, H.O. Kees, A. Ozcan, A. Khademhosseini, E. Haegstrom, D. Kuritzkes, U. Demirci, Integrating microfluidics and lensless imaging for point-of-care testing, *Biosensors and Bioelectronics* 24 (2009) 3208–3214.
 - [37] H. Zhu, O. Yaglidere, T.W. Su, D. Tseng, A. Ozcan, Cost-effective and compact wide-field fluorescent imaging on a cell-phone, *Lab on a Chip* 11 (2011) 315–322.
 - [38] H. Zhu, S. Mavandadi, A.F. Coskun, O. Yaglidere, A. Ozcan, Optofluidic fluorescent cytometry on a cell phone, *Analytical Chemistry* (2011).
 - [39] D.N. Breslauer, R.N. Maamari, N.A. Switz, W.A. Lam, D.A. Fletcher, Mobile phone based clinical microscopy for global health applications, *PLoS One* 4 (2009) e6320.
 - [40] Z. Iqbal, R.B. Bjorklund, Colorimetric analysis of water and sand samples performed on a mobile phone, *Talanta* 84 (2011) 1118–1123.
 - [41] D. Tseng, O. Mudanyali, C. Oztoprak, S.O. Isikman, I. Sencan, O. Yaglidere, A. Ozcan, Lensfree microscopy on a cellphone, *Lab on a Chip* 10 (2010) 1787–1792.
 - [42] S. Sun, J. Francis, K.E. Sapsford, Y. Kostov, A. Rasooly, Multi-wavelength spatial LED illumination based detector for in vitro detection of Botulinum neurotoxin A activity, *Sensors and Actuators B: Chemical* 146 (2010) 297–306.
 - [43] M. Yang, S. Sun, Y. Kostov, A. Rasooly, A simple 96 well microfluidic chip combined with visual and densitometry detection for resource-poor point of care testing, *Sensors and Actuators B: Chemical* 153 (1) (2011) 176–181.
 - [44] M. Yang, S. Sun, H.A. Bruck, Y. Kostov, A. Rasooly, Lab-on-a-chip for label free biological semiconductor analysis of Staphylococcal enterotoxin B, *Lab on a Chip* 10 (2010) 2534–2540.

Biographies

Joshua M. Balsam studied Mechanical Engineering at the University of Maryland (College Park, MD) and in 2009 received his BS in the field. In 2010 he began research in microfluidic biological sensors with Dr. Avraham Rasooly at the US Food and Drug Administration (FDA) in White Oak, MD. Currently he is an engineering PhD candidate at the University of Maryland under Dr. Hugh A Bruck, as well as a research assistant at the FDA in the Office of Science and Engineering Laboratories (OSEL), Division of Biology (DB). His work involves the development point of care biosensors for global health care initiatives.

Hugh A. Bruck received BS and MS in Mechanical Engineering in 1988 and 1989 respectively, and his PhD in Materials Science from Caltech in 1995. After working at Idaho National Engineering Laboratories, he came to the Department of Mechanical Engineering at the University of Maryland as an assistant professor in 1998 and is currently professor and associate chair for Academic Affairs working on functional materials and nanoscale property characterization. His current research has led to the development of a new combinatorial technique for formulating polymer nanocomposites and highly filled polymers, new processing-structure-property models for multifunctional polymer nanocomposites, new label-free biosensors based on electrical percolation and enhanced chemiluminescence in bio-nanocomposites, and new multiscale characterization approaches for hierarchically structured polymer composites and biological materials. He has authored or co-authored 9 book chapters, 70 journal papers, and 75 conference papers through support from ONR, AFOSR, NSF, FDA, ARO, ARL, NAVAIR, and NAVSEA. His work during that time has been recognized with many honors and awards, including the Best Paper Award at the 2011 ASME Mechanisms & Robotics Conference, A.J. Durelli Award, ONR Young Investigator Program Award, and Fulbright Scholar Award. He currently serves on the International Advisory Board for the *Journal Experimental Mechanics*, and was named a fellow of ASME in 2008.

Yordan Kostov holds BSc and MSc in Electrical Engineering and combined PhD degree in Electrical/Chemical Engineering. After post-doctoral studies in the Institute for Technical Chemistry, University of Hannover, Germany in 1994, he accepted a position as an assistant professor in the Department of Biotechnics, Sofia Technical University, Bulgaria. At present, he is research associate professor at the Center for Advanced Sensor Technology, University of Maryland, Baltimore County (UMBC). He is involved in the development of optical chemical and biochemical sensors.

Avraham Rasooly joined the Food and Drug Administration (FDA) as a Microbiologist in 1995, where he is developing microbial detection approaches for foodborne pathogens and their toxins using biosensors and DNA microarrays. Currently Dr. Rasooly holds a joint FDA Center for Devices and Radiological Health (CDRH) and National Cancer Institute (NCI) appointment, continuing his research technologies for biodetection at FDA and serving as a Branch Chief in the NCI's Center to Reduce Cancer Health Disparities (CRCHD).